

Model for the Bremsstrahlung Spectrum in EPMA. Application to Standardless Quantification

Jorge Trincavelli,* Gustavo Castellano and J. Alberto Riveros

Facultad de Matemática, Astronomía y Física, Universidad Nacional de Córdoba, Consejo Nacional de Investigaciones Científicas y Técnicas de la República Argentina, Fa.M.A.F., Ciudad Universitaria, 5000 Córdoba, Argentina

The Kramers expression was modified after fitting 52 spectra from targets of diverse composition at several incident energies. The function obtained describes adequately the continuum x-ray spectrum observed when a bulk, homogeneous and polished sample is irradiated by an electron beam with energies ranging from 5 to 35 keV. The targets considered are pure and multicomponent, covering elements from boron to bismuth. In addition to simplicity, the new expression shows very good agreement with measured spectra—much closer than other models assessed. The proposed function was applied to a standardless quantification method based on peak-to-background ratios.
© 1998 John Wiley & Sons, Ltd.

X-Ray Spectrom. 27, 81–86 (1998)

INTRODUCTION

Spectra from an electron microprobe consist of characteristic peaks superimposed upon a continuum spectrum ranging from very low energies up to the incidence energy E_0 . A good description of the continuum spectrum is of great interest in microanalysis, since an incorrect subtraction of this background may lead to important experimental errors. For this reason, an expression capable of describing the background for each spectrum to be processed becomes necessary. If an adequate functional form is known, a fit will produce the parameters corresponding to the experimental conditions of the considered spectrum.

In 1923, Kramers¹ proposed an expression for the continuum spectrum using a classical approximation in the calculation of the bremsstrahlung cross-section and the Thomson–Widdington law² for the stopping power. According to this description, the total intensity (number of photons per unit time) detected per incident electron with energies between E and $E + \Delta E$ when a sample of atomic number Z is irradiated with electrons of energy E_0 can be expressed as

$$\Delta I = FZ \frac{E_0 - E}{E} \Delta E \quad (1)$$

where the factor F involves the sample absorption of the observed radiation, the losses due to backscattering of electrons, the detection efficiency for energy E and geometric constants of detection.

This model is not suitable for microanalysis, although it has largely been used for describing the spectrum proceeding from an x-ray tube, where the most important region corresponds to energies greater than 5 keV due to the strong attenuation of low energies in the tube

window. For this reason, a number of modifications have been suggested to improve the description of experimental data in EPMA.

Lifshin³ suggested a correction factor to Eqn (1):

$$\Delta I = FZ \frac{E_0 - E}{E} [1 + a(E_0 - E)] \Delta E \quad (2)$$

and Reed⁴ proposed another modification also dependent on energy:

$$\Delta I = FZ \frac{E_0 - E}{E^{1+b}} \Delta E \quad (3)$$

In these two expressions a and b are constants.

Fiori *et al.*⁵ used Lifshin's expression to perform background subtraction in energy dispersive analysis. They suggested fitting the constants involved by considering two different energies in the continuum spectrum for which there are no characteristic photons.

Whilst Eqns (2) and (3) may be adequate to carry out a correct background subtraction in experimental spectra, they are not useful to predict spectra as a function of Z , E_0 and E . Since such a prediction is a basic requirement for quantifying by means of peak-to-background ratios, the expressions dependent on empirical parameters are not of interest in this context: the information desired is hidden precisely within these parameters.

Peak-to-background ratios have been a subject of investigation for the past 20 years, because they may allow one to develop an absolute analytical method since the continuum radiation generated in the sample can be considered as an internal standard. Although inaccurately known atomic parameters are involved, geometric effects of difficult determination are eliminated. Moreover, since the absorption of characteristic photons is similar to that suffered by continuum radiation, the requirements that must be imposed on the sample surface are reduced. This is an important advantage because it allows one to perform standardless

* Correspondence to: J. Trincavelli.

analysis as well as to extend the technique to rough samples, thin films, particles, etc.

Several workers have tried to find an analytical description for the experimental background so that only one parameter remained undetermined.^{6–8} This constant depends on the particular detection geometry and must be fitted for each equipment—but not for each spectrum because it is not related either to the sample composition or to the excitation conditions.

Statham⁶ calculated the constant b in Eqn (3) for certain elements (Al, Ti, Mn, Cu and Au), taking into account the anisotropy in bremsstrahlung generation—reflected in the dependence of b on the take-off angle. Thus, the continuum spectrum can be described for the five elements considered by Statham using b values calculated by him. Nevertheless, it should be borne in mind that, as calculations were performed for a particular value of E_0 (20 keV), any extrapolation to too different energies may be inadequate.

Smith and Gold⁷ obtained an analytical expression for the continuum spectrum as a function of Z , E and E_0 following a previous development by Rao-Sahib and Wittry:⁹

$$\Delta I = F \left(\frac{E_0 - E}{E} \right)^x Z^n \Delta E \quad (4)$$

where

$$n = E(0.0739 - 0.0051 \ln Z) + 1.6561 - 0.115 \ln Z$$

$$x = 1.76 - 0.00145Z/E$$

Small *et al.*⁸ observed that discrepancies between the existing models for bremsstrahlung and experimental values were about 50% or even 100%. For this reason they developed an expression by fitting a large set of experimental data:

$$\Delta I = F \left(Z \frac{E_0 - E}{E} \right)^M e^B \Delta E \quad (5)$$

where

$$M = 0.00599E_0 + 1.05$$

$$B = -0.0322E_0$$

Nevertheless, the predictions given by Eqn (5) are not accurate enough for a wide range of experimental conditions, particularly for high atomic numbers. In addition, when using this model in quantifying by means of an algorithm based on peak-to-background ratios,¹⁰ the results obtained are not satisfactory (see below). The lack of a reliable expression for predicting the continuum spectrum for a wide range of elements, incidence overvoltages and photon energies prompted the present work.

EXPERIMENTAL

The expression for the bremsstrahlung presented in this work was obtained by fitting a large set of spectra, involving samples of diverse Z , ranging from boron to bismuth, measured at several excitation energies in two different instruments: a JEOL-JXA 733 microprobe and a JSM-840 scanning microscope, both with energy-dispersive systems and Si(Li) detectors. The take-off angle was 40° in both cases.

The most important features of the spectra selected for performing the fit are shown in Table 1. An additional set of spectra was considered (Table 2) for evaluating the performance of the function obtained and for comparison with other models for the continuum spectrum.

In order to determine accurately the values of the incident energy E_0 , a careful calibration was carried out in order to find then the Duane–Hunt limit, i.e. the energy value for which the continuum intensity falls to zero. It must be emphasized that since there exists a non-zero probability of detecting sum photons because of pile-up counts in the detector, beyond the Duane–Hunt limit a region with non-zero intensity may be observed. This problem is avoided by observing the energy value for which the slope of the spectrum changes suddenly.

Finally, with the purpose of applying the obtained function to a peak-to-background ratio algorithm, a set of standard spherical particles was used (NBS K227).

Table 1. Spectra considered for performing the fit

Sample	Equipment	E_0 (keV)	t (s)	i (nA)
BN	JSM-840	5.35, 10.4, 15.55, 20.3, 25, 30	1000	1
Mg	JXA-733	25	100	1
Al	JXA-733	25	100	1
Ti	JXA-733	25	100	1
Fe	JXA-733	25	100	1
Cu	JXA-733	10, 15, 20.2, 25, 30	400	2
Zn	JXA-733	25	100	1
Mo	JXA-733	25	100	1
Ag	JXA-733	10.05, 15.1, 20.15, 38	400	2
Cd	JXA-733	25	100	1
Ta	JXA-733	11, 12.15, 13.15, 14.15, 15.15 17.2, 20.2, 23, 26, 30	500	2
Au	JXA-733	10.2, 12.4	400	2
Au	JXA-733	13.15, 14.15, 15.15, 16.2, 17.2 18.2, 20.25, 23, 25, 30, 35	500	2
Bi	JXA-733	15.1, 16.05, 17.1, 18, 20.05, 23 25, 30, 35, 38	400	2

Table 2. Spectra used for testing the expression obtained for the bremsstrahlung emission

Sample	Equipment	E_0 (keV)	t (s)	i (nA)
Apatite	JXA-733	25	60	1
Cr	JXA-733	25	100	1
Pb	JXA-733	14, 15, 16, 17, 18, 20, 23, 25, 30, 35, 38	400	2
Pt	JXA-733	13, 14, 15, 17, 18, 20, 23, 25, 30, 35,	500	2
Rh	JXA-733	25	1000	1
Si	JXA-733	5	150	2.65
Zr	JXA-733	25	100	1
Al ₂ O ₃	JSM-840	15	200	1.48
Albite	JSM-840	15	200	1.49
Apatite	JSM-840	15	200	1.464
CaF ₂	JSM-840	15	200	1.464
Fe	JSM-840	15	200	1.467
GaAs	JSM-840	15	200	1.467
GaP	JSM-840	15	200	1.467
Mg	JSM-840	15	200	1.464
MgO	JSM-840	15	200	1.464
Mn	JSM-840	15	200	1.467
Orthoclase	JSM-840	15	200	1.467
S ₂ Fe	JSM-840	15	200	1.48
SiO ₂	JSM-840	15	200	1.467
Ti	JSM-840	15	200	1.47
V	JSM-840	15	200	1.467
ZnS	JSM-840	15	200	1.467
Cr	JSM-840	6.3, 10.4	1000	0.121
Cr	JSM-840	20.5, 30	1000	0.06

These samples contain mainly lead, silicon and oxygen, and were measured in the JEOL JXA-733 microprobe, with a beam current of 2 nA, an incident energy of 25 keV and live times from 200 to 400 s.

DATA REDUCTION AND ANALYSIS

The experimental data used for describing the global behavior of the continuum spectrum were chosen with the intention of including a wide range of atomic numbers (6–83) and incident energies (5–35 keV), so that general situations in microanalysis were covered. The spectrum of boron nitride was included to guarantee a good description of bremsstrahlung for elements such as carbon and oxygen, which often appear in usual EPMA applications.

In each of the selected spectra, the very low energies were excluded ($E < 1$ keV), as well as channels containing peaks (characteristic, escape peaks, sum peaks and internal Si fluorescence). These peakless spectral regions were corrected for absorption, backscattering loss and detection efficiency, thus converting to continuum spectra generated in each sample. The whole set of data was then fitted, taking Z , E_0 and E as independent variables.

Absorption correction

Although the energy dependence of the bremsstrahlung cross-section is different from that corresponding to ionization, the differences are partially masked because

of electron straggling in the target. Therefore, it is a reasonable assumption to consider the depth distribution of continuum x-ray production to be similar to that of characteristic radiation. Hence, the path that both types of radiation must traverse within the sample is the same, and the absorption correction for the bremsstrahlung radiation of a given energy can be approximated as that corresponding to characteristic photons of the same energy. This is a usual assumption when dealing with the description of the generated continuum spectrum,^{7,8} and will also be taken as valid for the present analysis. It should be noted that this approximation might lose validity on changing the detection geometry. In the present work, fits and comparisons were performed for a take-off angle of 40°, which is a typical array for normal incidence.

The absorption correction used in this work is based on the ionization depth distribution function given by Packwood and Brown¹¹ with coefficients modified by Riveros *et al.*¹² In the case of continuum radiation, it must be taken into account that an electron is capable of producing bremsstrahlung photons of energy E provided its energy is higher than E , whereas for characteristic radiation the critical excitation energy is the minimum energy of interest. Mass absorption coefficients were calculated with the expression given by Heinrich.¹³

Backscattering correction

A fraction of the incident electrons escapes the sample with enough energy to produce further bremsstrahlung; hence, an additional factor R_c must account for these backscattering losses. This factor is included in the parameter F in Eqns (1–5).

In this work, the expression given by Statham¹⁴ was used for R_c . This model is a function of the backscattering correction R_{ch} for characteristic photons. The expression used for R_{ch} was that given by Love *et al.*¹⁵

Detection efficiency correction

The fraction of photons collected by the detector depends on the thicknesses of its different components: beryllium window, gold layer, silicon dead layer and, to a lesser extent, detector active thickness. The correct knowledge of the first three is often a problem, since the manufacturers' specifications are not always complete. For this reason, a careful analysis of the influence of the different thicknesses was performed. The effect of photon attenuation at the different detector layers was observed to be restricted to energies very close to each absorption edge. Therefore, it was possible to vary separately each thickness in order to achieve a good approach for the real values. This procedure was performed by means of an exhaustive analysis of spectra free of characteristic peaks in the region of interest.

During the present work, the JSM-840 microscope detector was repaired between two different sets of measurements, its characteristic thicknesses being modified; as a result, it worked as a detector of different efficiency after the repair. Data corresponding to the 'three' detectors are given in Table 3.

Table 3. Characteristic thicknesses of the detectors used in this work^a

Detector	X_{Be} (μm)	X_{Au} (μm)	X_{DL} (μm)	X_{det} (mm)
JXA-733	12.5	0.02	0.1	5
JSM-840	17.5	0.01	0.2	3
JSM-840 ^b	9	0.01	0.1	3

^a X_{Be} , X_{Au} , X_{DL} and X_{det} correspond to beryllium window, gold layer, dead layer and active thickness, respectively.

^bThicknesses of the JSM-840 microscope's detector after repair.

Data processing

Kramers' model¹ has been used by several workers as a basis for a more realistic expression of the continuum radiation, because it is a simple function with some theoretical support and gives a functional approximation to the bremsstrahlung spectrum. These features led to it being used as a starting point to build up an empirical model in the present work, with the purpose of describing adequately experimental data over a wide range of Z , E_0 and E .

According to Kramers' equation [Eqn (1)], the intensity I of photons of energy E generated within the sample per energy interval, without correcting for back-scattering losses, can be expressed as

$$I \propto Z \frac{E_0 - E}{E} \quad (6)$$

The first step for processing the data was to fit a plane to a dependent variable:

$$Y = \frac{IE}{Z(E_0 - E)} \quad (7)$$

as a function of Z , E_0 and E for the whole set of experimental values. After fitting, a marked dependence on Z was still found. In order to solve this problem, the variable Y was modified by adding an exponent to the atomic number. Finally, it was observed that the fits improved when this exponent was around 0.5, resulting in a plane as a function of $\ln Z$, E_0 and E . With this, the expression obtained for the generated intensity is

$$I = \sqrt{Z} \frac{E_0 - E}{E} \times (-52.22 - 1.462E + 0.515E_0 + 29.27 \ln Z) \quad (8)$$

Before obtaining this equation, spectra measured with the JXA-733 were used, which led to an equation similar to Eqn (8); then I values measured with the JSM-840 were normalized, i.e. the constant that relates the solid angles subtended by both detectors was determined. Channels corresponding to $E > 4$ keV were considered, so that the detection efficiency did not influence the determination of the normalization factor. Thus, a constant was fitted to each spectrum measured with the JSM-840; all the constants obtained were very similar and the average value was taken as the normalization factor. By re-scaling the spectra measured with the JSM-840 with this factor, the database was enlarged and then a new fit was performed, giving Eqn (8).

The equation obtained appeared very appropriate to describe most of the spectra considered in the fitting (Table 1), in addition to a number of additional spectra used for testing Eqn (8) (Table 2). Slight deviations arose only for very high values of E_0 and Z (Bi at 35 and 38 keV and Pb at 38 keV) and low atomic numbers. The differences observed for $Z > 80$ at $E_0 \geq 35$ keV are acceptable as they are limiting cases in EPMA. Nevertheless, discrepancies found for low atomic numbers cannot be neglected, since light elements are major constituents in a number of important applications of the technique. In order to overcome this inconvenience, a set of boron nitride spectra was included in the database used to perform the fit, looking for a function able to improve the description for light elements and keeping the good performance for medium and high atomic numbers. Adding a new term dependent on Z and E_0 to Eqn (8), the following expression was fitted:

$$I = \sqrt{Z} \frac{E_0 - E}{E} \times \left(-54.86 - 1.072E + 0.2835E_0 + 30.4 \ln Z + \frac{875}{Z^2 E_0^{0.08}} \right) \quad (9)$$

When dealing with multielement targets, the bremsstrahlung production I of all the elements must be averaged. Since each contribution is proportional to bremsstrahlung atomic cross-sections, the average should be weighted with the corresponding atomic fractions. However, as this effect influences spectrum predictions very weakly, replacement of Z in Eqn (9) by a mean value results a very good approximation.

COMPARISON WITH OTHER MODELS

In order to give a magnitude for the deviations in the intensity predictions I with respect to the experimental data \tilde{I} , a value for χ^2 was calculated for each spectrum:

$$\chi^2 = \frac{1}{N} \sum_{i=1}^N \frac{(I_i - \tilde{I}_i)^2}{\tilde{I}_i} \quad (10)$$

where i denotes each of the N channels in the spectrum considered. In order to obtain a global value for χ^2 , an average is assessed, weighting each χ^2 with the number of channels of the corresponding spectrum.

As mentioned above, Kramers' expression¹ is inadequate to describe the functional behavior of I for the whole range considered for E_0 , E and Z ; on the other hand, Lifshin's model³ does not give a global prediction for the bremsstrahlung, but requires a particular fit for each spectrum—a clear disadvantage if the continuum is intended to be described as a function of the three mentioned variables. Regarding the equation given by Smith and Gold,⁷ Small *et al.*⁸ have shown that its performance is very deficient. The expression given by Reed⁴ has the same limitations as Lifshin's, but Statham⁶ determined values for the 'constant' b in Eqn (3) for certain elements (see Introduction).

In order to compare Eqn (9) with Reed's model, a subset S of spectra was selected, corresponding to those elements for which Statham fitted the parameter b ; using Eqn (3) with these values, a single value for the scaling factor included in F was determined. Since this model is optimized for predicting spectra for this limited number of elements, a comparison with the global expression given in Eqn (9) favors the Reed–Statham equation. However, Table 4 shows a better performance of the model developed in this work. A comparison with Eqn (5) given by Small *et al.*⁸ is also shown, now including the whole set of data (Tables 1 and 2). A scaling factor was also fitted in this case.

Although the primary intention of this work is an adequate description of generated bremsstrahlung within the sample, it is interesting to study the behavior of the different correction models (absorption and backscattering) included in factor F . The present model achieves a better performance with the factor F used for

the fitting than with any other, as expected. However, in addition, it must be emphasized that the expression given by Small *et al.*⁸ also shows a better performance when including this model for F instead of that used originally (see Table 4 and Fig. 1).

The performances of the different models are shown in Table 4; spectra have also been grouped by atomic number, in order to appreciate the limitations of each model. It can be seen that the model presented here has a better performance than any other in all sets of data, even in the subset S containing only those elements for which Statham⁶ gave the constant b in Eqn (3). On the other hand, the expression of Small *et al.*⁸ gives reasonable predictions for low and intermediate Z , whilst it is not recommended for $Z \geq 45$. In Fig. 1, the expressions obtained in this work and that of Small *et al.*⁸ are compared with experimental spectra for BN at 20 keV, MgO at 15 keV, Cu at 20 keV and Pb at 25 keV. As can be seen, the equation given by Small *et al.*⁸ gives poorer descriptions of experimental data for high Z , whereas for low Z the advantage of the present model is not so important, except for BN, for which the differences are again large.

Table 4. χ^2 values for the different models compared: present work, Reed⁴ with coefficients given by Statham,⁶ Small *et al.*⁸ with absorption and backscattering corrections given in the original work and with those included in the model proposed here (Small-F)

χ^2	Subset S (6015 data)	Whole set (35361 data)	$Z < 45$ (21091 data)	$Z \geq 45$ (14270 data)
This work	4.3	4.1	2.6	6.3
Statham	9.9	—	—	—
Small	150	99	6.3	240
Small-F	97	65	5.3	150

APPLICATION TO STANDARDLESS QUANTIFICATION

Here the expression proposed in this work is used in a standardless quantification. The algorithm employed is based on peak-to-background ratios¹⁰ and was applied to a set of standard spherical particles with the composition given in Table 5. These particles were grouped

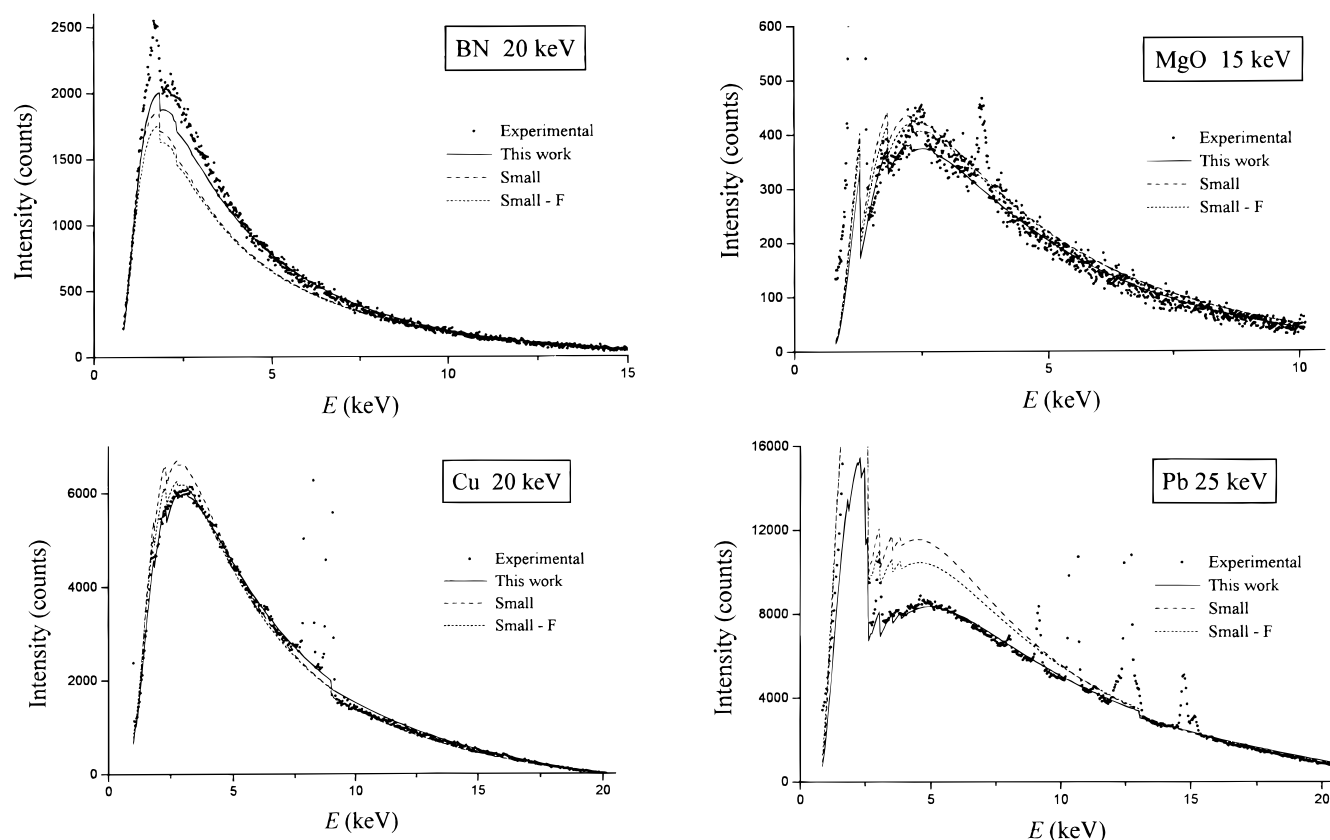


Figure 1. Comparison of the different models for bremsstrahlung spectrum with experimental data.

Table 5. Concentrations obtained by a peak-to-background standardless algorithm¹⁰ using the model for bremsstrahlung proposed in this work and the model given by Small *et al.*,⁸ and certified values^a

		Group 1 <i>d</i> = 1–2 μm	Group 2 <i>d</i> = 2–3 μm	Group 3 <i>d</i> = 3–4 μm	Group 4 <i>d</i> = 4–7 μm	Certified value
Pb (%)	This work	77 ± 2	74 ± 1	74 ± 2	72 ± 2	74.3
	Small	71 ± 3	67 ± 1	67 ± 2	65 ± 2	
Si (%)	This work	8.3 ± 0.9	9.5 ± 0.4	9.4 ± 0.8	10.0 ± 0.8	9.0
	Small	11 ± 1	12.0 ± 0.5	12.0 ± 0.9	12.6 ± 0.9	
O (%)	This work	15 ± 1	16.6 ± 0.8	16.5 ± 1	17.5 ± 1	16.3
	Small	19 ± 2	21.0 ± 0.9	21 ± 2	22 ± 2	

^a Particles were divided into four groups according to their diameter *d*. Each average value given corresponds to about 10 particles.

according to their diameters: 1–2 μm (group 1), 2–3 μm (group 2), 3–4 μm (group 3), 4–7 μm (group 4). Each group is composed of about 10 particles.

A better performance of the model for bremsstrahlung proposed here compared with the expression given by Small *et al.*⁸ is shown in Table 5. It might be expected that uncertainties in the prediction of bremsstrahlung would cancel when normalizing to 100%; nevertheless, differences between concentrations determined by means of the model of Small *et al.*⁸ and the certified values can be clearly appreciated.

CONCLUSION

The model developed for predicting bremsstrahlung is a simple analytical function of *Z*, *E*₀ and *E*. It was obtained after fitting a large and diverse set of experi-

mental data. The resulting expression shows very good agreement with spectra measured over a wide range of experimental conditions, much closer than with other published models.

The expression proposed not only is a powerful tool for background subtraction in EPMA, but also shows important advantages when included in a standardless quantification algorithm based on peak-to-background ratios.

Acknowledgements

The authors thank Professor Van Grieken for his assistance when performing experimental work at the University of Antwerp (UIA). They are also grateful to the Serveis Científico-Tècnics of the Universitat de Barcelona, where the measurements were completed. Finally, they acknowledge financial support from the Consejo Nacional de Investigaciones Científicas y Técnicas de la República Argentina.

REFERENCES

1. H. Kramers, *Philos. Mag.* **46**, 836 (1923).
2. R. Widdington, *Proc. F. London, Ser. A* **86**, 360 (1912).
3. E. Lifshin, in *Proceedings of the 9th Annual Conference of the Microbeam Analysis Society*, Ottawa, Canada (174), No. 53 (1974).
4. S. Reed, *X-Ray Spectrom.* **2**, 16 (1975).
5. C. Fiori, R. Myklebust, K. Heinrich and H. Yakowitz, *Anal. Chem.* **48**, 233 (1976).
6. P. Statham, *X-Ray Spectrom.* **5**, 154 (1976).
7. D. Smith and C. Gold, *X-Ray Spectrom.* **4**, 149 (1975).
8. J. Small, S. Leigh, D. Newbury and R. Myklebust, *J. Appl. Phys.* **61**, 2, 459 (1987).
9. T. Rao-Sahib and D. Wittry, in *Proceedings of the 6th International Conference on X-Ray Optics and Microanalysis*, edited by G. Shinoda, K. Kohra and T. Ichinokawa, p. 131. University of Tokyo, Tokyo (1972).
10. J. Trincavelli and R. Van Grieken, *X-Ray Spectrom.* **23**, 254 (1994).
11. R. Packwood and J. Brown, *X-Ray Spectrom.* **10**, 138 (1981).
12. J. Riveros, G. Castellano and J. Trincavelli, *Mikrochim. Acta, Suppl.* **12**, 99 (1992).
13. K. Heinrich, presented at the IX Australian Symposium on Analytical Chemistry, Sydney (1987).
14. P. Statham, *Proc. Annu. Conf. Microbeam Anal. Soc.* **14**, 247 (1979).
15. G. Love, M. Cox and V. Scott, *J. Phys. D* **11**, 7 (1978)